Mean lifetime of the bound $2p\sigma$ state of HeH^{2+}

I. Ben-Itzhak,[1] Z. Chen,[1] B. D. Esry,[1] I. Gertner,[2] O. Heber,[2,*] C. D. Lin,[1] and B. Rosner[2]
[1]*James R. Macdonald Laboratory, Department of Physics, Kansas State University, Manhattan, Kansas 66506*
[2]*Department of Physics, Technion, Haifa 32000, Israel*
(Received 1 October 1993)

Recently, experimental evidence for the existence of a bound state of the HeH^{2+} molecular ion was reported by Ben-Itzhak, Gertner, Heber, and Rosner [Phys. Rev. Lett. **71**, 1347 (1993)]. This three-body system was predicted by Bates and Carson to have bound vibrational states in the $2p\sigma$ electronic state despite the strong repulsion potential between the two nuclei. These $2p\sigma$ vibrational states decay via an electronic transition to the $1s\sigma$ repulsive ground state with a mean lifetime of about 1 nsec. We have used the "fragment-fragment" coincidence method to measure the mean lifetime of the HeH^{2+} molecular ions which dissociate in flight before reaching the detector. The yield of these molecular ions was measured as a function of the distance between the target cell and the analyzer exit. From this measurement a mean lifetime of 3.9 ± 0.4 nsec was determined. The $2p\sigma \rightarrow 1s\sigma$ transition rates for all vibrational states have been calculated within the Born-Oppenheimer approximation using available oscillator strengths. It is shown that the transition rates decrease with increasing vibrational energy because of the "stretch" of the molecular ion. The distribution of $2p\sigma$ vibrational states populated by vertical transitions from stripping the HeH^{+} electronic ground state was evaluated, and the resulting decay curve compares well with the measured one.

PACS number(s): 34.50.Gb, 35.80.+s

I. INTRODUCTION

Three-body problems have been of increasing interest in the last few years, especially for three charged particles where the interaction between them is well known [1–9]. The Schrödinger equation for one-electron molecular ions is separable in confocal elliptical coordinates within the Born-Oppenheimer approximation. Thus molecular ions, like H_2^+ and HeH^{2+}, are a good testing ground for improving our understanding of few-body problems. Three-body systems with two light particles like the He atom are more complicated because one cannot use the Born-Oppenheimer approximation. This effect of the masses of the three interacting particles was studied from the He atomic limit (one heavy particle) to the H_2^+ molecular limit (one light particle) by Chen and Lin [1]. The effect of increasing the strength of the attractive potential in the Hamiltonian is studied using heliumlike ions with increasing Z. On the other hand, increasing the repulsive potential term in the Hamiltonian generally results in an unbound system which can be studied only by scattering methods. The asymmetric HeH^{2+} molecular ion for which some states have been predicted to be bound by Bates and Carson [2] and by Winter, Duncan, and Lane [3] is an exception to this trend. The energy curves of the two lowest electronic states obtained within the Born-Oppenheimer approximation are shown in Fig. 1. For this molecular ion, the large repulsion between the two nuclei causes the $1s\sigma$ ground state and most of the other electronic states of HeH^{2+} to be repulsive. The lowest attractive potential curve is the $2p\sigma$ first excited electronic state. It has a minimum 0.849 eV deep at $R_0=3.89$ a.u. which can sustain 15 vibrational states.

The mean lifetime of the $2p\sigma$ state is expected to be short because it can decay by an electronic transition to

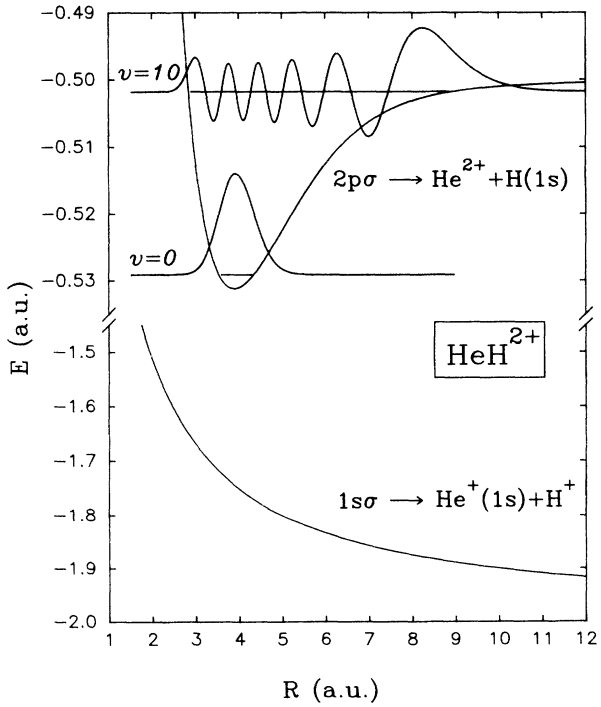

FIG. 1. Potential-energy curves for HeH^{2+} (zero corresponds to $He^{2+}+H^{+}+e$).

*Permanent address: Department of Nuclear Physics, Weizmann Institute of Science, Rehovot 76100, Israel.

the repulsive $1s\sigma$ ground state. The oscillator strength of this transition, as well as other transitions between low HeH^{2+} states, have been calculated by Arthurs, Bond, and Hyslop [4]. The mean lifetime of the $2p\sigma$ bound state can be calculated using the well-known spontaneous decay rate formula [10]

$$\tau^{-1}=W_{ka}^{s}=\frac{2\omega_{ka}^{2}}{mc^{3}}|f_{ka}|F^{2}\ , \tag{1}$$

where $F=|\int\psi_{v'}^{*}\psi_{v}dR|$ is the Frank-Condon factor. Using the transition frequency $\omega_{ka}(R_0)\sim 1.22$ a.u. and oscillator strength $f_{ka}(R_0)=0.0250$ given by Arthurs, Bond, and Hyslop [4] and assuming that the Frank-Condon factor is approximately one, the mean lifetime is estimated to be about 1 nsec.

Recently, we have reported experimental evidence of the formation of the bound $2p\sigma$ electronic state of HeH^{2+} molecular ions [11,12]. These ions were produced in charge-stripping collisions of 0.9-MeV HeH^{+} with Ar gas. The measurement of the mean lifetime of the HeH^{2+} molecular ion is an experimental challenge because it travels only a few mm in one mean lifetime. In Sec. II of this paper we report the measurements of the mean lifetime of the $2p\sigma$ state of HeH^{2+}, using the "fragment-fragment" coincidence method. We have also calculated the decay rate of the $2p\sigma\rightarrow 1s\sigma$ electronic transitions and found that they depend on the vibrational state of the HeH^{2+} molecular ion as discussed in Sec. III. The measured and calculated mean lifetimes are compared to one another in Sec. IV.

II. EXPERIMENTAL METHOD

The experimental method used for determining the mean lifetime is somewhat similar to the one used for the detection of the bound HeH^{2+} molecular ions [11,12]. A HeH^{+} beam with an energy of 900 keV, the highest energy available at the Technion Van de Graaff accelerator, was used. At this beam energy, the ions' speed is about 6 mm/nsec. The experimental setup, shown in Fig. 2, consisted of a short target cell (6 mm), with small entrance and exit collimators (0.5 and 1.0 mm diameters, respectively), in which the HeH^{+} projectiles collided with a thin Ar target ($P\sim 2$ mTorr). The ions produced in these collisions were analyzed according to their mass-to-charge ratio by a strong magnetic field (~ 0.8 T) in the narrow gap between two small permanent magnets (having a 12.7 mm diameter). This small analyzing magnet was mounted on a high-precision translation stage such that its distance from the target cell could be varied over the range of 40 mm. Special care was taken to ensure that the magnetic field direction remained vertical when the magnets were moved. The trajectories of the ions passing through this analyzer are determined within a time range of up to 10 nsec from the moment of their production. During these short flight times the number of $HeH^{2+}(2p\sigma)$ molecular ions is expected to decrease significantly. This reduction in the HeH^{2+} yield with increasing distance traveled by the ions was used to determine their mean lifetime.

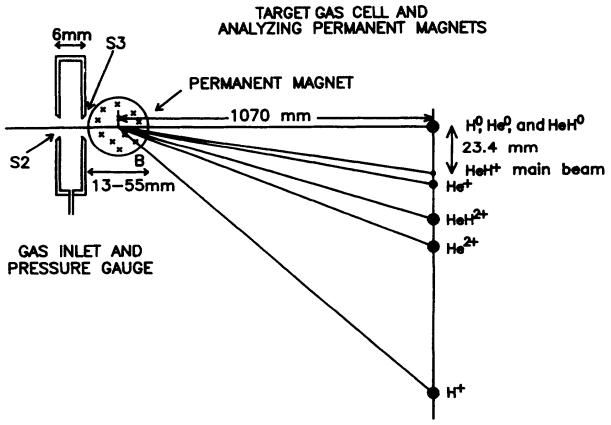

FIG. 2. Experimental setup and schematic trajectories of the different ions after the analyzing magnet.

The analyzed ions are detected (with 100% efficiency) by a surface barrier detector 1070 mm down stream. An iris aperture in front of the detector defines the angular resolution of the system to be about 0.3°, big enough to collect all the fragments. The position of this detector can be changed relative to the beam axis so that the yield of the different ions can be measured as a function of the deflection angle. Another surface barrier detector, with a 0.5-mm-diam collimator, is placed on the beam axis for normalization. The trajectories of the different ions are well separated as shown in Fig. 2. The HeH^{2+} molecular ions which have passed through the magnetic field before they have dissociated are deflected by an angle of 2.5°. The flight time to the detector is of the order of 180 nsec, thus no $HeH^{2+}(2p\sigma)$ molecular ions are expected to reach it.

The ions that hit the surface barrier detector produce signals proportional to their energy. Hydrogen fragments should therefore peak at 20% of the beam energy while the He fragments should peak at 80% of the beam energy. (The fragments have approximately the beam velocity, thus their energy is proportional to their mass.) These peaks are clearly seen in the energy spectrum taken at 2.5° shown in Fig. 3. Furthermore, in cases where both the hydrogen and the helium fragments hit the detector simultaneously, the full energy of the beam will be deposited in the detector. These "fragment-fragment" coincidence events contribute to the full energy peak, also shown in the figure.

We have used "fragment-fragment" coincidences as a signature of the formation of bound states of HeH^{2+} [12]. The $H^{+}+He^{+}$ fragments follow approximately the trajectory of the HeH^{2+} molecular ions if the dissociation happens after the magnetic field. This trajectory is well resolved from the trajectories of the other ions which were produced before the magnet, as can be seen in Fig. 2. The deviations from the HeH^{2+} trajectory caused by the "Coulomb explosion" of the molecule are small as the beam energy is orders of magnitude larger than the energy released in the dissociation. These $H^{+}+He^{+}$ coincidence events are recorded under the full energy peak shown in Fig. 3, and they indicate that HeH^{2+} ions have passed through the analyzing magnet before dissociation.

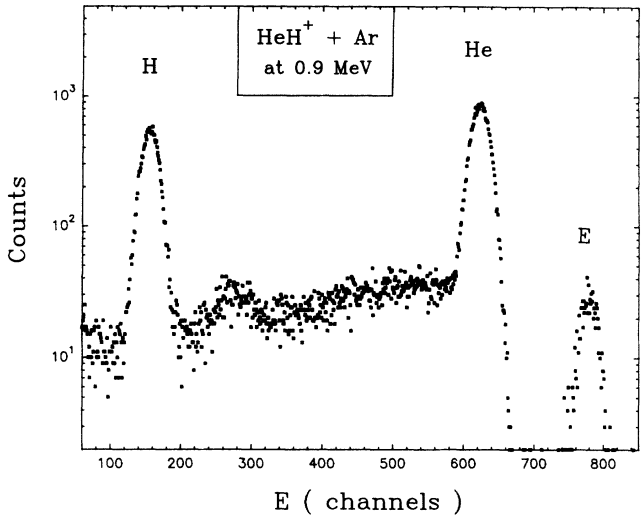

FIG. 3. Energy spectrum of the ions hitting the detector placed on the HeH^{2+} trajectory. The full energy peak labeled by E is associated with both the H and He fragments hitting the detector simultaneously.

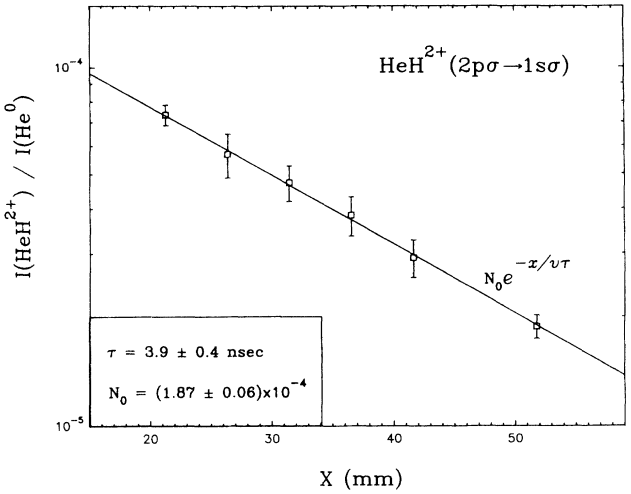

FIG. 4. Normalized number of coincidence events as a function of the distance between the target cell and the magnet exit. The solid line is a fit of a single exponential to the data which yields $\tau_{expt}=3.9\pm0.4$ nsec.

In order to determine the mean lifetime of the bound $2p\sigma$ states of HeH^{2+}, we have measured the number of $H^+ + He^+$ coincidence events normalized to a constant number of neutral helium fragments as a function of the distance x between the target cell and the analyzing magnet exit. These coincidence events are the number of HeH^{2+} molecular ions which survived all the way up to the magnet exit for each distance x. To ensure that this is the true coincidence rate, the number of these coincidences was measured at each distance as a function of the deflection angle. At the deflection angles where the coincidence rate peaks, the random coincidence rate is practically zero, as was discussed in detail in our previous publications [11,12].

The normalized $H^+ + He^+$ coincidence yield, plotted in Fig. 4, decreases with increasing distance between the target cell and the magnet exit. A single exponential decay fits this data nicely, giving a mean lifetime of

$$\tau_{expt}=3.9\pm0.4 \text{ nsec} . \quad (2)$$

This experimental value is about a factor of 4 larger than the value estimated from the calculated electronic decay rate at R_0. Such a large deviation from the estimated 1 nsec is unexpected if one assumes that the only difference between the decay rates of the vibrational states is due to Franck-Condon factors.

Now that the mean lifetime of $HeH^{2+}(2p\sigma)$ is known, the cross section for its production can be evaluated from the previously measured apparent cross section [12]. In order to evaluate the total production cross section, we have measured the yield of $HeH^{2+}(2p\sigma)$ relative to the neutral He fragments, shown in Fig. 5(a). This ratio is practically independent of the target pressure, and its value is $R=(2.25\pm0.30)\times10^{-4}$. The yield of the neutral He fragments relative to the main HeH^+ beam was also measured as a function of pressure. Using the slope of this linear pressure dependence, shown in Fig. 5(b), the apparent cross section for $HeH^{2+}(2p\sigma)$ production (i.e., the cross section for formation and survival of these molecular ions) was evaluated to be

$$\sigma_{ap}=\frac{R\times\left[\text{slope}\left[\frac{I(He^0)}{I(HeH^+)}\right]\right]}{3.54\times10^{13}l_T}$$
$$=(1.8\pm0.3)\times10^{-20}\text{ cm}^2 , \quad (3)$$

where $l_T=0.6$ cm is the target length. As both the apparent cross section and the mean lifetime are known now, the true production cross section can be determined. The typical flight time of the HeH^{2+} molecular ions to the exit of the analyzer is $t=3.6\pm0.5$ nsec, depending on where in the target cell they were formed. Thus only a fraction of these molecular ions, $f=e^{-t/\tau}=0.40\pm0.07$, makes it through the analyzer and contributes to the $H^+ + He^+$ coincidence yield. The total production cross section is then given by

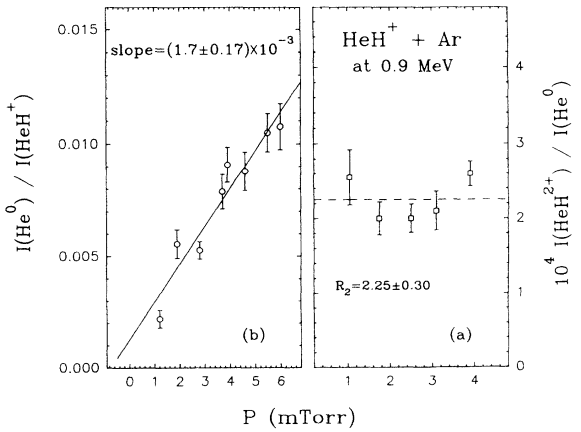

FIG. 5. The ratios of (a) $I(HeH^{2+})/I(He^0)$ and (b) $I(He^0)/I(HeH^+)$ as a function of target pressure.

$$\sigma=\sigma_{ap}/f=(4.5\pm1.1)\times10^{-20}\ \text{cm}^2\ . \quad (4)$$

This value is an order of magnitude smaller than the previously reported rough estimate [12] because the measured mean lifetime is significantly longer than the previously estimated 1 nsec.

III. THEORY

The decay of $HeH^{2+}(2p\sigma)$ molecular ions is predicted theoretically to proceed via an electronic transition to the $HeH^{2+}(1s\sigma)$ repulsive ground state, which then dissociates rapidly into $H^+ + He^+$. The potential-energy curves of the HeH^{2+} molecular ion are known analytically from the application of the Born-Oppenheimer approximation. This approximation is also expected to be valid during the electronic transitions which are faster than the nuclear motion. The electronic spontaneous decay rate W^s_{ka} at a fixed internuclear distance R is given by

$$W^s_{ka}(R)=\frac{2}{c^3}\omega^2_{ka}(R)f_{ka}(R)\ , \quad (5)$$

where $\omega_{ka}(R)=E_{2p\sigma}(R)-E_{1s\sigma}(R)$ is the transition frequency, $f_{ka}(R)$ is the oscillator strength, and k and a are the initial $2p\sigma$ and final $1s\sigma$ electronic states, respectively. To evaluate the expectation value of the electronic spontaneous decay rate from any vibrational state one must average over all possible internuclear distances, the probability of which vs the internuclear distance is given by $|\psi_v(R)|^2$. Within this simple model the $2p\sigma\rightarrow1s\sigma$ decay rate is given for each vibrational state by

$$\lambda_v=\overline{W^s_{ka}}=\int_0^\infty W^s_{ka}(R)|\psi_{v_{2p\sigma}}(R)|^2dR\ . \quad (6)$$

The decay rate can be calculated for each vibrational state bound in the $2p\sigma$ electronic state using the oscillator strength $f_{ka}(R)$ calculated previously by Arthurs, Bond, and Hyslop [4]. Since they presented values for the oscillator strength only for the region $R\leq5.0$ a.u., it was necessary to extrapolate to large values of R which are needed in order to evaluate the integral in Eq. (6). A simple exponential fit, $f_{ka}(R)=ae^{-bR}$, of the last five points from Arthurs, Bond, and Hyslop [4] was used with $a=0.5882$ and $b=0.8077$. It was also necessary to interpolate in between the given points to obtain a sufficient density of points for the numerical integration (a cubic spline fit was used.) Once the decay rate was calculated using Eqs. (5) and (6) the mean lifetime of each vibrational state can easily be obtained using the relationship $\tau_v=1/\lambda_v$. The mean lifetimes calculated in this manner do not depend strongly on the extrapolation and interpolation procedures. Performing these calculations using an oscillator strength f_{ka} extrapolated by fitting the last three to nine points gave a variation of less than $\pm0.05\%$ for the mean lifetime of the lowest state and less than $\pm3.1\%$ for the highest state. The interpolated and extrapolated f_{ka} is also shown in Fig. 6.

The vibrational wave functions bound in the $2p\sigma$ electronic state of HeH^{2+} were evaluated using the finite-differences method [13]. Using these numerical wave functions the decay rates have been calculated for the different vibrational states. The mean lifetimes slowly increase with increasing vibrational quantum number for low values of v as shown in Fig. 7. On the other hand, for highly excited vibrational states they increase rapidly. The experimental value of $\tau_{expt}=3.9\pm0.4$ nsec is close to the theoretical value, $\tau_{10}=3.4$ nsec, of the $v=10$ state.

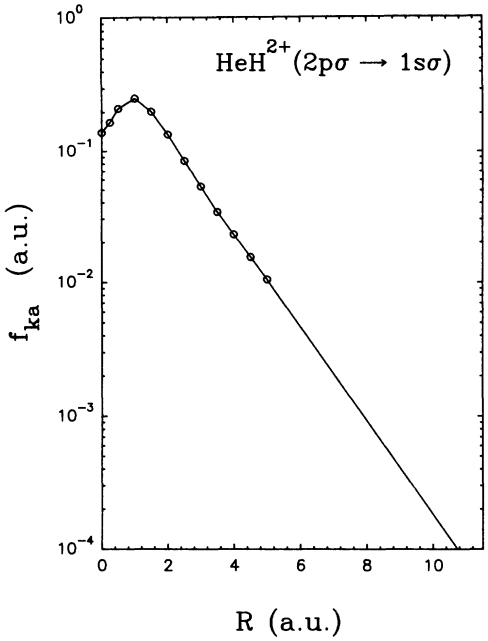

FIG. 6. The oscillator strength $f_{ka}(R)$ (symbols from Ref. [4]) for the $2p\sigma\rightarrow1s\sigma$ dipole transitions as a function of the internuclear separation R showing also the interpolation and extrapolation (lines).

The dipole transition amplitude, in the Born-Oppenheimer approximation which is valid for the $2p\sigma\rightarrow1s\sigma$ electronic transitions, can be written as

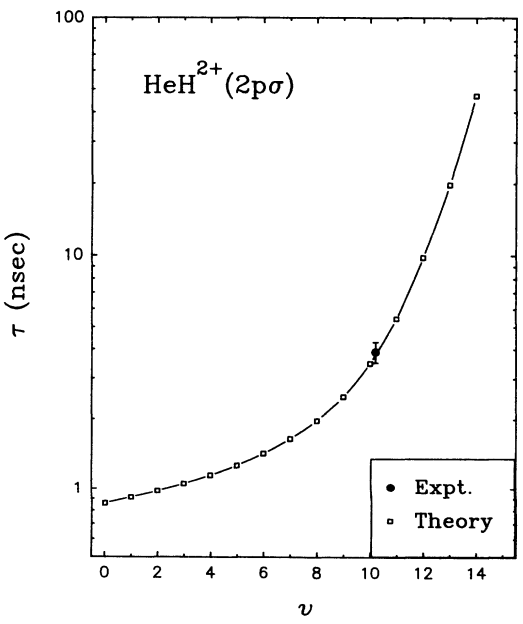

FIG. 7. The mean lifetimes of the different vibrational states of $HeH^{2+}(2p\sigma)$.

$$\int_0^\infty \psi^*_{v_{1s\sigma}}(R) D_{\rm el}(R) \psi_{v_{2p\sigma}}(R) dR \ , \tag{7}$$

where the integration over the coordinates of the electron is separated from the integration over the internuclear distance, resulting in an electronic transition amplitude at each R given by

$$D_{\rm el}(R) = \int_0^\infty \phi^*_{1s\sigma}(R;\mathbf{r}_e) \mathbf{D} \phi_{2p\sigma}(R;\mathbf{r}_e) d\mathbf{r}_e \ , \tag{8}$$

$\phi(R;\mathbf{r}_e)$ is the electronic wave function and $\psi_v(R)$ is the nuclear vibrational wave function. In the commonly used Franck-Condon approximation, one assumes that $D_{\rm el}(R)$ is independent of R which then separates the transition amplitude into a product of the average electronic transition amplitude and the Frank-Condon factor, the overlap integral between the initial and final vibrational states,

$$\bar{D}_{\rm el} \int_0^\infty \psi^*_{v_{1s\sigma}}(R) \psi_{v_{2p\sigma}}(R) dR \ , \tag{9}$$

where $\bar{D}_{\rm el}$ is the average value of $D_{\rm el}(R)$ given in Eq. (8).

The electronic transition decay rates from bound to repulsive states are expected to depend only weakly on the vibrational state if the Franck-Condon principle holds. This is because the overlap integrals with continuum wave functions typically do not change significantly even on a relatively large range of internuclear distances. But, for highly excited vibrational states of HeH^{2+}, which are expected to play a major role in the collisions under study as will be discussed later in this paper, the wave functions extend over a large range of internuclear distances. Thus the Franck-Condon approximation, i.e., $D_{\rm el}(R) \sim \bar{D}_{\rm el}$, is not expected to be valid.

The fast decrease of the $2p\sigma \rightarrow 1s\sigma$ electronic decay rate with increasing internuclear separation R is a result of the difference between the electronic densities of the two states involved. The electron density of the $2p\sigma$ state is centered mostly on the proton, while the $1s\sigma$ density is centered mostly on the α particle as shown schematically in Fig. 8. At small R values there is still some electron density on the other center (the α particle for $2p\sigma$ and the proton for $1s\sigma$) so that the transition amplitude is nonzero; but, as the separation between the two centers increases, one expects an exponential decrease in the value of these transition amplitudes. Thus transitions between these two electronic states are practically impossible unless the internuclear distance is small. The low-lying vibrational states for which only R values around R_0 are important will not be affected, but the highly excited vibrational states which have a large probability at large R values will have a much smaller decay rate. The highly excited vibrational states of $HeH^{2+}(2p\sigma)$ are an example of the breakdown of the Franck-Condon approximation even though the Born-Oppenheimer approximation is still valid, i.e., a vertical transition does not necessarily mean that the electronic transition amplitude is independent of R. As most transitions commonly studies are from low vibrational states of narrow potential wells, one grows accustomed to the fact that the Born-Oppenheimer and the Franck-Condon approximations are simultaneously valid for vertical transitions, even though this is not always the case.

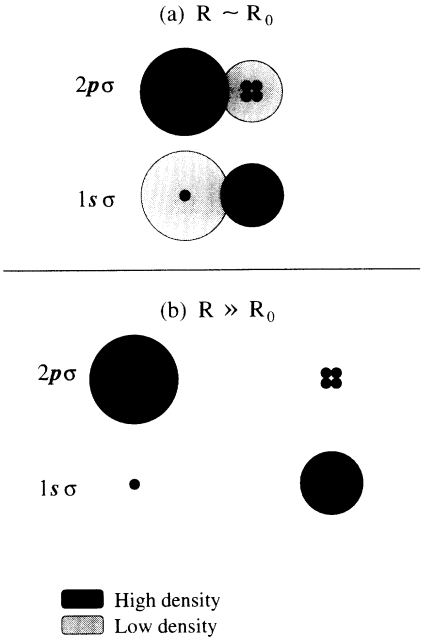

FIG. 8. Schematic electronic density distribution of the $2p\sigma$ and $1s\sigma$ states at (a) small and (b) large internuclear distances (darker shade is a higher density).

IV. RESULTS AND DISCUSSION

The mean lifetime of the HeH^{2+} molecular ions was evaluated from the direct measurement of their yield as a function of the distance traveled from the target cell, where they were formed by charge-stripping collisions, to the exit of the analyzing magnet. In these collisions of 0.9-MeV HeH^+ with Ar gas, the only bound electronic state of HeH^{2+} populated is the $2p\sigma$ as was reported previously [12]. This electronic state of HeH^{2+} decays via an electronic transition to the $HeH^{2+}(1s\sigma)$ repulsive ground state, which then dissociates rapidly into $H^+ + He^+$. The measured mean lifetime of this electronic state was determined to be 3.9 ± 0.4 nsec, as shown in Fig. 4. Furthermore, from the figure it can be seen that any significant deviation from this single exponential decay line will be in clear disagreement with the data.

The calculated mean lifetimes for the different vibrational states, presented in Fig. 7, vary significantly from one highly excited state to the other. The experimental value is close to the calculated value of the $v = 10$ state. But, one may question why such highly excited vibrational states of the HeH^{2+} are preferentially populated, and what would be the effect of a broad distribution of these vibrational states on the expected mean lifetime? In order to answer the above questions, a better understanding of the whole process is needed: starting with the formation of HeH^+ molecular ions in the rf source of the accelerator, going through the $HeH^+ + Ar \rightarrow HeH^{2+}$ vertical transitions during the fast charge-stripping collisions, and ending with the $2p\sigma \rightarrow 1s\sigma$ spontaneous electronic transitions.

The population of vibrational states of HeH^+ and other ions formed in rf sources, similar to the one used in the

Technion accelerator, have been studied, for example, by Kanter *et al.* [14] and Zajfman *et al.* [15]. It has been shown that a Boltzmann distribution is obtained with an effective temperature T_{eff} which depends on the type of the ion source and its operating parameters. Thus it is reasonable to assume that the HeH^+ beam has a Boltzmann distribution of vibrational states given by

$$P(v_i) \propto e^{-(E_{v_i}-E_0)/kT_{\text{eff}}}, \tag{10}$$

where E_v and E_0 are the energies of the vibrational state with quantum number v and of the lowest vibrational state, respectively. For the typically low temperatures in the source, most of the HeH^+ molecular ions are in their vibrational ground state.

During the fast charge-stripping collision with the Ar target ($t_{\text{coll}} \sim 10^{-17}$ sec), the nuclear motion can be neglected. These transitions are commonly described as vertical transitions from the initial $HeH^+(^1\Sigma^+)$ electronic ground state to the final $HeH^{2+}(2p\sigma)$ electronic state as shown in Fig. 9. Under these conditions, the transition rates between the different initial and final vibrational states are given approximately by the square of the Franck-Condon factors,

$$T(v_i \rightarrow v_f) = \left| \int_0^\infty \psi^*_{v_f}(R)\psi_{v_i}(R)dR \right|^2, \tag{11}$$

where $\psi_{v_i}(R)$ and $\psi_{v_f}(R)$ are the initial and final vibrational wave function, respectively. The initial wave functions have been evaluated using the finite differences method with the HeH^+ ground-state potential reported by Kolos and Peek [16]. Using the numerical vibrational wave functions of HeH^+ and HeH^{2+}, the transition rates have been calculated between all initial and final states. For example, the transition rates from some initial vibrational states, $v_i = 0$, 2, and 4, to all final states are plotted in Fig. 10 normalized as a probability distribution. It can be clearly seen that the distribution of final states shifts toward lower vibrational states if one starts from a higher initial vibrational state. Thus a high effective temperature of the HeH^+ beam, which has a higher fraction of highly excited states, will create a distribution of final vibrational states centered around a lower vibrational state of HeH^{2+}. This final vibrational state population can be determined once the transition rates are known by summing over all initial vibrational states

$$P(v_f) = \sum_{v_i} P(v_i)T(v_i \rightarrow v_f). \tag{12}$$

In Fig. 11 the distribution of vibrational states of HeH^{2+} created from a HeH^+ beam with $T_{\text{eff}} = 500$ K is presented as an example. A wide distribution peaked around $v_f = 9$ is the result of such collisions. Mostly highly excited vibrational states are populated because of the large difference between the HeH^+ and HeH^{2+} equilibrium distances. This difference makes the overlap integrals,

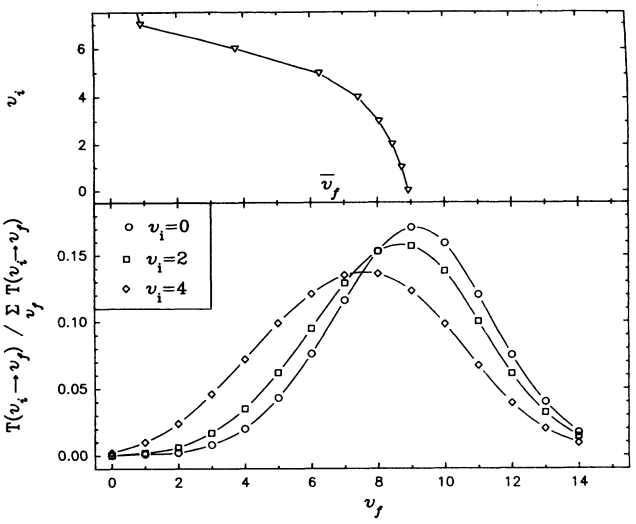

FIG. 10. (a) Final population of vibrational states of $HeH^{2+}(2p\sigma)$ produced from some initial vibrational states of $HeH^+(^1\Sigma^+)$ ($v_i = 0$, 2, and 4). (b) The average final vibrational state of $HeH^{2+}(2p\sigma)$ as a function of the initial vibrational state of $HeH^+(^1\Sigma^+)$.

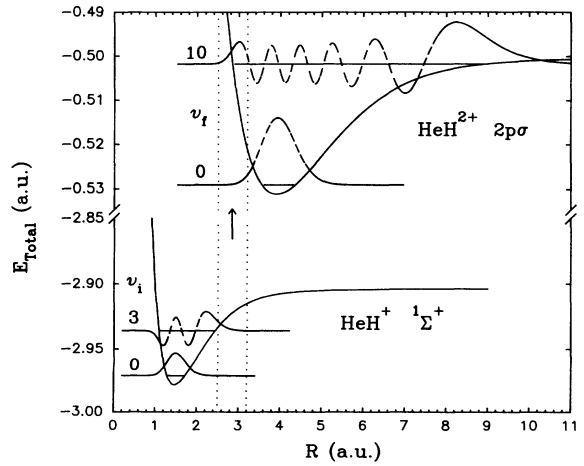

FIG. 9. Potential-energy curves for the electronic ground state of HeH^+ (from Ref. [15]) and the lowest bound state of HeH^{2+} (from Ref. [2]).

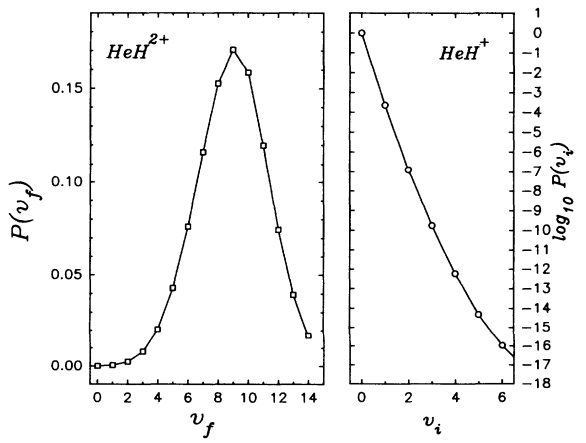

FIG. 11. The population of initial vibrational states of $HeH^+(^1\Sigma^+)$ at $T_{\text{eff}} = 500$ K and the resulting final population of vibrational states of $HeH^{2+}(2p\sigma)$.

Eq. (11), between two low-lying states extremely small. On the other hand, the wave functions of the highly excited states extend over a large range of R, resulting in significantly larger overlap integrals.

For the effective temperature discussed above, only a few vibrational states are expected to have significant contributions to the mean lifetime measurement. The fraction of HeH^{2+} molecular ions surviving after a given flight time for a given population of final vibrational states is given by

$$\frac{N(t)}{N_0}=\sum_{v_f} P(v_f)e^{-t/\tau_{v_f}}, \tag{13}$$

where $P(v_f)$ is the population of final vibrational states of $HeH^{2+}(2p\sigma)$ calculated from Eq. (12) and τ_{v_f} are the mean lifetimes of the different vibrational states discussed in the preceding section. Even though the bound $HeH^{2+}(2p\sigma)$ molecular ions are produced with a narrow distribution of R in the vertical transitions during the collision, they have a wide distribution of R when they spontaneously decay. This is because the typical vibration time ($\sim 10^{13}-10^{-14}$ nsec) is orders of magnitude smaller than the mean lifetime of the $2p\sigma$ state of HeH^{2+}. This molecular ion "forgets" the initial R distribution so that the final R distribution is well described by its vibrational wave function.

The number of HeH^{2+} molecular ions as a function of their flight time from the target cell to the analyzing magnet exit are shown in Fig. 12. The solid line represents the best χ^2 fit to the data, for which $T_{\text{eff}}=1530$ K (N_0 and T_{eff} are the only free parameters in our calculations). The dashed line is the single exponential fit discussed in the experimental section which yields a mean lifetime of 3.9±0.4 nsec. Both lines are in very good agreement with the experimental data. Further measurements over a wider range of flight times are needed in order to determine which model fits the data better: a single exponential decay curve or our model calculation. The theoretical model developed to explain our experimental results resolved the "apparent discrepancy" between our earlier mean lifetime estimate and the measured value. These calculations indicate that the $2p\sigma \rightarrow 1s\sigma$ electronic decay rate has a strong dependence on the vibrational state of the HeH^{2+}, especially for highly excited states. This can be better understood if one uses the following simple qualitative picture. The electronic decay rate falls off rapidly with increasing internuclear separation R, as can be seen from Fig. 6. This rapidly changing oscillator strength is due to the fact that the electron density of the $2p\sigma$ state for large values of R is centered mostly on H while for the $1s\sigma$ it is centered mostly on He^+ for large values of R. This makes transitions between these two electronic states practically impossible unless the internuclear distance is small. Now, higher vibrational levels are "stretched" over a wider range of R, with a larger probability of being found at large R values. But, when R is large, the probability for an electronic transition is negligible. As a result of this reduction in transition probability the mean lifetime of these highly excited states will be longer. In fact, the highest vibrational state has a mean lifetime of nearly 50 nsec. Our calculations also suggest that the HeH^{2+} measured mean lifetime depends on the initial population of vibrational states of the HeH^+ molecular ions in their electronic ground state. Thus similar experiments performed using different experimental systems might lead to different results mainly due to the difference in the effective temperature in the ion source. Future experiments are planned to test the sensitivity of the measured mean lifetime of $HeH^{2+}(2p\sigma)$ to the effective temperature of the HeH^+ molecular ions. For such experiments better control and understanding of the rf source is needed.

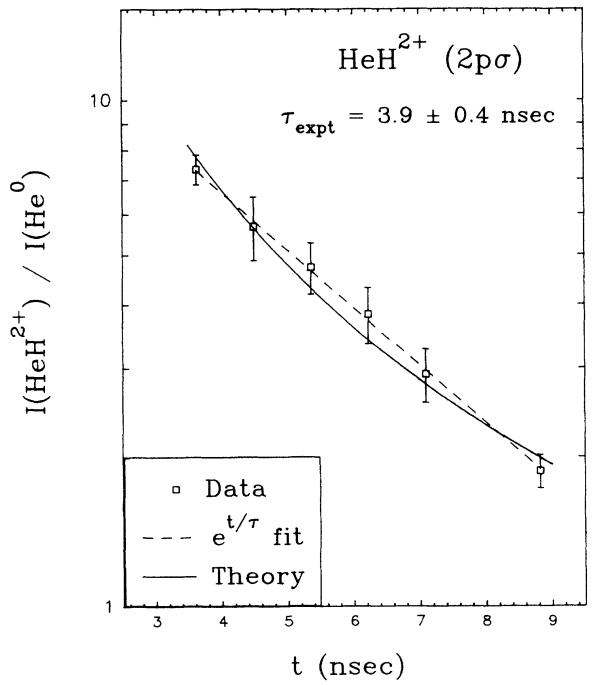

FIG. 12. The ratio of HeH^{2+} to He^0 as a function of the flight time from the target cell to the magnet exit. The solid line is the model calculation for an effective temperature of 1530 K in the ion source. The dashed line is a single exponential decay fit to the data with $\tau_{\text{expt}}=3.9\pm0.4$ nsec.

V. SUMMARY

The mean lifetime of the $2p\sigma$ electronic state of HeH^{2+} has been measured to be 3.9±0.4 nsec from the dependence of the "fragment-fragment" coincidence rate on the distance between the target cell and the analyzer exit. A distribution of $2p\sigma$ vibrational states is populated in the $HeH^+ + Ar$ collisions by vertical transitions from the HeH^+ electronic ground state. These vibrational states of the $2p\sigma$ bound state decay by electronic transitions to the $1s\sigma$ repulsive ground state, the decay rates of which have been calculated using available oscillator strengths. The population of final vibrational states produced in the charge-stripping collisions decays as a superposition of exponentials at a rate which reproduces the measured yield of HeH^{2+} molecular ions as a function of their flight time. These electronic transition rates of the

different vibrational states of the $HeH^{2+}(2p\sigma)$ decrease with increasing vibrational energy because of the "stretch" of the molecular ions. The Franck-Condon principle is not valid for these decays because of the wide range of internuclear separations involved and the different density distribution of the states involved [over this range $D_{el}(R)$ changes by more than an order of magnitude—it is not even "approximately" constant], thus demonstrating that vertical transitions do not necessarily mean that the transition rates depend mostly on the overlap integrals.

ACKNOWLEDGMENTS

We wish to thank J. Saban, H. Shemi, and A. Sternberg for their invaluable technical assistance. We also wish to thank Professor O. L. Weaver, Professor K. D. Carnes, and Dr. V. Krishnamurthi for useful discussions. This work was supported in part by the Foundation for Promotion of Research at the Technion and in part by the Division of Chemical Sciences, Office of Basic Energy Sciences, Office of Energy Research, U.S. Department of Energy.

[1] Z. Chen and C. D. Lin, Phys. Rev. A **42**, 18 (1990).
[2] D. R. Bates and T. R. Carson, Proc. R. Soc. London, Ser. A **234**, 207 (1956).
[3] T. G. Winter, M. D. Duncan, and N. F. Lane, J. Phys. B **10**, 285 (1977).
[4] A. M. Arthurs, R. A. B. Bond, and J. Hyslop, Proc. R. Soc. London, Ser. A **70**, 617 (1957); A. M. Arthurs and J. Hyslop, *ibid.* **70**, 489 (1957).
[5] K. Helfrich, Z. Phys. D **13**, 295 (1989).
[6] Chi-Yu Hu, A. A. Kvitsinsky, and S. P. Merkuriev, Phys. Rev. A **45**, 2723 (1992).
[7] Armin Scrinzi, Phys. Rev. A **45**, 7787 (1992).
[8] M. I. Haftel and V. B. Mandelzweig, Phys. Rev. A **46**, 142 (1992).
[9] H. T. Coelho, J. J. De Groote, and J. E. Hornos, Phys. Rev. A **46**, 5443 (1992).
[10] B. H. Bransden and C. J. Joachain, *Physics of Atoms and Molecules* (Longman, New York, 1983).
[11] I. Ben-Itzhak, I. Gertner, and B. Rosner, in *The Physics of Highly Charged Ions,* edited by P. Richaud, M. Stockli, C. L. Cocke, and C. D. Lin, AIP Conf. Proc. No. 274 (AIP, New York, 1993), p. 214.
[12] I. Ben-Itzhak, I. Gertner, O. Heber, and B. Rosner, Phys. Rev. Lett. **71**, 1347 (1993).
[13] W. H. Press, S. A. Teukolsky, W. T. Vetterling, and B. P. Flannery, *Numerical Recipes in FORTRAN,* 2nd ed. (Cambridge University Press, Cambridge, England, 1992).
[14] E. P. Kanter, P. J. Cooney, D. S. Gemmell, K. O. Groeneveld, W. J. Pietsch, A. J. Ratkowski, Z. Vager, and B. J. Zabransky, Phys. Rev. A **20**, 834 (1979).
[15] D. Zajfman, E. P. Kanter, Z. Vager, and J. Zajfman, Phys. Rev. A **43**, 1608 (1991).
[16] W. Kolos and J. M. Peek, Chem. Phys. **12**, 381 (1976).

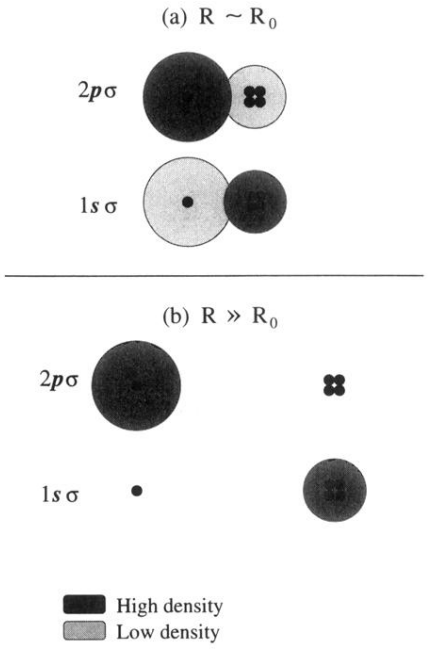

FIG. 8. Schematic electronic density distribution of the $2p\sigma$ and $1s\sigma$ states at (a) small and (b) large internuclear distances (darker shade is a higher density).